P2B.3 **IMPROVEMENT OF WSR-88D VAD WINDS: CYCLONIC WIND FIELDS**

Vincent T. Wood
NOAA/OAR/National Severe Storms Laboratory
Norman, Oklahoma

1. INTRODUCTION

Hurricanes pose a serious threat to life and property along the Gulf and Atlantic coastal regions of the United States. The Weather Surveillance Radars-1988 Doppler (WSR-88D) network provides the potential to improve hurricane forecasts and warnings by monitoring changes in a hurricane's track, eye diameter, radar eyewall and rainband reflectivities. The WSR-88D Velocity-Azimuth Display (VAD) Wind Profile (VWP) display is a useful tool for diagnosis of wind fields at different altitudes as a hurricane is approaching a coastal WSR-88D.

Vertical profiles of wind are routine products on the WSR-88D network. These winds are obtained from the VAD technique (Lhermitte and Atlas 1961; Rabin and Zrnic 1980) and are available whenever backscattering is sufficient to produce detectable signals. The technique is based on the assumption that the zeroth and first harmonic are obtained from the Fourier least squares fit and the power of higher harmonics can be neglected.

Figure 1 presents the WSR-88D VAD wind profiles derived from the operational VAD algorithm (O'Bannon 1985) as Hurricane Katrina approached the New Orleans/Slidell WSR-88D (KLIX) on 29 August 2005. The hurricane center was located about 30 n mi (56 km) to the east-southeast (about 160º) of the radar. KLIX reflectivity and velocity displays at low elevation angles at 1300 UTC on this day are shown in Fig. 2. In spite of the fact that there was strong radar return within 10-25 n mi (19-46 km) of the radar where VAD winds were derived, there were many missing winds at different heights and also the non-missing winds had large root-mean-square (RMS) values shown in Fig. 1. The wind vectors are colored according to the RMS differences in the lower-right portion of the figure.

The objectives of this paper are: (a) to investigate why many missing winds occur and non-missing winds have large RMS values when there are strong radar returns and good Doppler velocity data and (b) to present a new solution to recover or improve VAD winds as a hurricane approaches a coastal WSR-88D. A Doppler radar simulation is used by Wood and Brown (1992) to explain how the simulated sine curves change as a simulated hurricane approaches the WSR-88D.

2. CURVED WIND FIELD ACROSS VAD CIRCLE

VAD plots were prepared for all the VWP heights at 1300 UTC (Fig. 1). Representative samples of the plots are shown in Fig. 3. It is evident that all of the plots have a common feature – Doppler velocity peaks around the VAD are not 180º apart. They change from 110º to 160º apart on the side toward the hurricane center; they vary from 200º to 250º apart on the opposite side. The azimuthal variations of Doppler velocity measurements depart from a Fourier first-order sine curve. At 1300 UTC, the lack of fit of the sine curve to the data results in RMS differences greater than a velocity threshold value of 9.7 kt (5 m s^{-1}) at all heights below 30 kft (9 km), except at 9 kft (2.7 km) and 14 kft (4.3 km) where the RMS differences are 8.5 kt (4.4 m s^{-1}) and 8.6 kt (4.4 m s^{-1}), respectively (Figs. 1 and 3). The threshold is one of the adjustable parameters that is specified for the existing WSR-88D VAD Algorithm (FHM-11, Part C; VAD Algorithm Description). Since the RMS difference exceeds the threshold, the computation of wind speed and direction would not be representative of the ambient winds. In this situation, ND (no data) is plotted on the VWP display (Fig. 1). Therefore, only the 9- and 14-kft wind vectors and most of missing winds appear below 30 kft on the VWP display at 1300 UTC.

In the next section, we propose a new solution to recover or improve VAD winds.

3. APPROACH

a. WSR-88D radar emulator

In order to understand why the quasi-sine curve distributed on the VAD circle does not match closely with the Fourier first-order sine curve (e.g., Fig. 3), WSR-88D Doppler velocity measurements of a model hurricane were simulated using a Doppler radar emulator that reproduced the basic characteristics of a WSR-88D (Wood and Brown 1992). Fig. 4 reveals how the quasi-sine curves vary as the hurricane approaches a coastal WSR-88D. When the hurricane center is located at far range south of the radar, the wind field is nearly uniform with winds blowing from east to west (Fig. 4a). It can easily be seen that extreme Doppler data points are ideally 180º apart (Fig. 4b).

As the hurricane approaches the radar, the azimuthal variation of Doppler velocity measurements increasingly departs from a first-order sine curve, because the extreme Doppler velocity values are dominated by the hurricane's circulation (Figs. 4c-4f). With decreasing range from the radar, the Doppler velocity patterns become distorted relative to the patterns at farther range (e.g., Wood and Brown 1992). The values around the VAD circle are less than 180º apart. The lack of fit of the first-order sine curve to the

Corresponding author address: Vincent T. Wood, National Severe Storms Laboratory, 120 David L. Boren Blvd., Norman, OK 73072. E-mail: Vincent.Wood@noaa.gov

simulated data results in increased RMS differences that exceed the threshold value of 9.7 kt (5 m s^{-1}).

b. Polynomial regression technique

There are a number of mathematical methods that may provide a solution for solving the problem described above. A higher-order Fourier least-squares fit could be applied; however, it does not perform well in the missing-data case, because it suffers from low resolution, aliasing, lack of data points around the VAD circle, and poor accuracy problems.

An alternative method for approximation may be based upon polynomials obtained by least-squares. A technique employs least-squares fit of the Doppler velocity data distributed on the VAD circle by successive polynomials of order n = 1, 2, etc. If $\tilde{V}_i$ is the i^{th} observed Doppler velocity value, our task is to minimize the sum of squares

$$J = \sum_{i=1}^{m} (V_i - \tilde{V}_i)^2 . \qquad (1)$$

Here, m is the total number of $\tilde{V}_i$ data points distributed on the VAD circle, and V_i is the model Doppler velocity value which may be expressed in terms of a polynomial regression (Carnahan et al. 1969) as

$$V_i = \sum_{j=0}^{n} b_j P_j , \qquad (2)$$

where b_j is the regression coefficients. P_j is the j^{th}-order polynomial in ϕ such that $P_0 = \phi^1$, $P_1 = \phi^2$, …, $P_n = \phi^{n+1}$, where ϕ represents the azimuth angle in radians. Differentiating (1) with respect to b_j (i.e., $\partial J / \partial b_k = 0$ for $k =$ 0, 1, 2, …, n) yields

$$\sum_{j=0}^{n} b_j \sum_{i=1}^{m} P_{ik} P_{ij} = \sum_{i=1}^{m} P_{ik} V_i , \qquad (3)$$

where P_{ij} is the value of the polynomial P_j evaluated at the i^{th} data value ϕ_i. In a matrix form, (3) becomes

$$\mathbf{b}\mathbf{P}^{\mathrm{T}}\mathbf{P} = \mathbf{P}^{\mathrm{T}}\mathbf{V} , \qquad (4)$$

which has the solution

$$\mathbf{b} = (\mathbf{P}^{\mathrm{T}}\mathbf{P})^{-1}\mathbf{P}^{\mathrm{T}}\mathbf{V} . \qquad (5)$$

In (4), the vectors $\mathbf{b} = \left[b_0 b_1 ... b_n\right]^{\mathrm{T}}$, $\mathbf{V} = \left[V_1 V_2 ... V_m\right]^{\mathrm{T}}$, and

$$\mathbf{P} = \begin{bmatrix} P_{10} & P_{11} & \cdots & P_{1n} \\ P_{20} & P_{21} & \cdots & P_{2n} \\ \vdots & \vdots & \ddots & \vdots \\ P_{m0} & P_{m1} & \cdots & P_{mn} \end{bmatrix} .$$

The RMS difference between the polynomial fit data (V_i) and the observed Doppler velocity values ($\tilde{V}_i$) is defined as

$$RMS = \left[\frac{1}{N} \sum_{i=1}^{N} (V_i - \tilde{V}_i)^2 \right]^{1/2} . \qquad (6)$$

Mean wind speed (WS) is computed from the average of the magnitudes of the positive and negative Doppler velocity peaks on the VAD circle and is given by

$$WS = (V_{\max} - V_{\min}) / 2 . \qquad (7)$$

Mean wind direction (WD) is determined from the average of the magnitudes of maximum and minimum azimuths, respectively, and is given by

$$WD = (\phi_{\min} + \phi_{\max}) / 2 - \pi / 2 , \qquad (8)$$

where $\phi_{\min}$ is the azimuth at which $V_{\min}$ occurs, and $\phi_{\max}$ is the azimuth at which $V_{\max}$ occurs. Eq. (8) is different from the computation of wind direction in the existing WSR-88D VAD algorithm. In the algorithm, wind direction is determined only from the azimuth of the negative peak of the sine curve, which is not correct for a curved flow, because the algorithm assumes uniform wind (i.e., constant wind direction and speed) along the VAD circle. Since the extreme positive and negative Doppler velocity values around the VAD circle are generally less than 180° apart, Eq. (8) is recommended, whether the flow is straight or curved. Wind at a given time and height is plotted on the VWP display using conventional wind barb notation.

4. EXPERIMENTAL VAD ALGORITHM

A number of adjustable parameters are specified for the existing WSR-88D VAD Algorithm (FHM-11, Part C; VAD Algorithm Description). An experimental VAD (XVAD) algorithm, similar to the WSR-88D VAD Algorithm, was developed with Eqs. (5)-(8), and a few new default values were added to the XVAD algorithm. The algorithm consists of the following steps. Actual Doppler velocity values during the approach of Hurricane Katrina at 1300 UTC on 29 August 2005 are plotted as a function of azimuth on the XVAD display at 9 kft (indicated by gray dots in Fig. 5). If the number of Doppler velocity data points is less than the minimum number of data points threshold (MIN_NOBS_THRES, default value of 25 points), then wind speed and direction will not be computed so that they are set to missing data parameter (default value of 999.0) and no data (ND) is plotted on the experimental VWP (XVWP) display.

If there are enough data points, the next task is to sort out the data points in order of increasing azimuths before performing a polynomial technique, via (5). The 6th order polynomial regression is performed (FIT =1), and a calculated RMS is returned as a result. The reason for choosing the 6th order is to keep the fitted curve from having too many maxima and minima distributed on the XVAD circle.

The next task is to determine whether noisy/bad data points are filtered out or not. If the RMS difference is less than the RMS threshold (RMS_VEL_THRES_1, default value of 8 kt), the remaining data points from the regression line are saved, as indicated by blue dots in Fig. 5. Other remaining data points (gray dots) more than 8 kt from the regression line are separated from the blue dots.

The next task is to perform the looping (4 times) of the polynomial regression starting from 7th order to10th order, until the RMS difference is less than 4 kt. If the RMS difference is less than the RMS threshold (RMS_VEL_THRES_2, default value of 4 kt), then a new polynomial regression curve is fitted to the remaining data points (FIT = 2), as shown by red dots in Fig. 5. The reason for defining the default value of 4 kt is a desire to plot a green wind vector on the VWP display. If the RMS difference still exceeds RMS_VEL_THRES_2 and the number of terms equals to the 10th order at the end of the looping, then no improvement has been obtained and the remaining data points (blue dots) are still available for next determining whether the quasi-sine curve is symmetrical or not. The quasi-sine curve is the vertical offset or the height of the baseline of the curve and is computed as

$$V_{vert\_shft} = (V_{\min} + V_{\max}) / 2 \,. \qquad (10)$$

When V_{vert_shft} (indicated by green horizontal line in Fig. 5) increases from zero Doppler velocity, the curve departs from symmetry, owing to (a) component of precipitation fall velocities, (b) divergence/convergence, and/or (c) improperly dealiased Doppler velocity values. If the offset exceeds the symmetry threshold (SYM_THRES, default of 13 kt), then there is a bad fit and BD (bad data) is plotted on the VWP display. “NOT SYMMETRY” is labeled. Otherwise, “SYMMETRY” is labeled, indicating that the curve is symmetric if the offset is less than the threshold (e.g., Fig. 5).

5. EXPERIMENTAL VWP DISPLAYS

a. Hurricane Katrina of 23-30 August 2005

On 29 August 2005, Hurricane Katrina was a large and intense hurricane that struck a portion of the United States coastline along the northern Gulf of Mexico (Knabb et al. 2005a). After reaching Category 5 intensity over the central Gulf of Mexico, Katrina weakened to Category 3 before making landfall on the northern Gulf coast. WSR-88D KLIX reflectivity and Doppler velocity displays at 1300 UTC on this day are shown in Fig. 2.

Figure 6 presents the XVAD wind profile (XVWP) derived from the XVAD algorithm using a higher-order polynomial regression technique. Nonmissing VAD-derived winds shown in Fig. 1, in spite of large RMS values, closely agree well with those in Fig. 6. In the latter figure, the deduced winds were from east-northeast at all heights. The polynomial regression XVAD curve fits the measurements with low RMS difference values. Table 1 presents the comparison of wind directions and speeds between the existing WSR-88D VAD Algorithm and the XVAD algorithm at 1300 UTC shown in Fig. 1. Note the erroneous wind directions derived from the WSR-88D VAD Algorithm, owing to the assumption of uniform winds distributed around the VAD circle.

Overall, the XVWP display (Fig. 6) indicated that Katrina already began weakening slowly from 1230 UTC to 1330 UTC.

b. Hurricane Rita of 18-26 September 2005

Rita remained a tropical storm with maximum winds of 60 kt (31 m s^{-1}) into the morning of 20 September 2005 as it approached toward the Florida Straits (Knabb et al. 2005b). Rita began to strengthen, and it became a hurricane with an intensity of 70 kt (36 m s^{-1}) by 1200 UTC 20 September about 100 n mi (185 km) east-southeast of Key West, Florida. While proceeding westward into the southeastern Gulf of Mexico, Rita then attained an intensity of 85 kt (44 m s^{-1}, Category 2) by 1800 UTC that day, and its center passed about 40 n mi (75 km) south of Key West about an hour later.

The Key West WSR-88D (KBYX) reflectivity and Doppler velocity displays of Hurricane Rita are presented in Fig. 7. Rita was located about 40 n mi to the south-southeast (about 170º) of the radar at 1731 UTC. Overlaid range-folded echoes (magenta) on the Doppler velocity display were spotty, including those within 50 n mi (93 km) and within the eye.

Figure 8 presents the WSR-88D VAD wind profile (VWP) derived from the operational VAD algorithm. There are so many missing winds considering that there were sufficient detactable signals, especially within 25 n mi of the radar where VAD winds were derived. When Rita was near the radar, the extreme Doppler velocity values were dominated by the hurricane’s circulation so that the azimuthal variation of Doppler velocity measurements depart from the first-order sine curve. The lack of fit of the curve to the data resulted in RMS differences greater than the threshold value at low-to-mid-altitudes.

Figure 9 shows the XVWP derived from the XVAD algorithm. The RMS differences are less than 4 kt at nearly all heights. Non-missing, operational VAD-derived winds (Fig. 8) are in good agreement with winds based on polynomial regression technique with low RMS differences (Fig. 9). At 50 kft (15 km), there are erroneous wind vectors, owing due to the lack of data points distributed uniformly on the XVAD circle. This is a problem that the XVAD cannot handle.

6. CONCLUSIONS

A higher-order polynomial regression technique was developed to employ a least-squares fit of the Doppler velocity data distributed on the XVAD circle by successive nth order polynomials. The technique did a good job of fitting the quasi-sinusoidal variation of

Doppler velocity values distributed on the XVAD circle. It is recommended that the XVAD algorithm be tested with more Doppler velocity data of other hurricanes.

7. ACKNOWLEDGMENTS

The author would like to thank Rodger Brown of NSSL and Randy Steadham of WSR-88D Radar Operations Center (ROC) for reading and making suggestions in this paper. Richard Murnan and Dave Zittel of WSR-88D ROC provided information about the characteristics of WSR-88Ds. Eddie Forren and Karen Cooper of NSSL provided technical expertise in implementing the tools and ensuring that the author had access to the data. This work was funded through a memorandum of understanding between NSSL and WSR-88D ROC.

8. REFERENCES

Carnahan, B., H. A. Luther, and J. O. Wilkes, 1969: *Applied Numerical Methods.* John Wiley and Sons, 604 pp.

Knabb, R. D., J. R. Rhome, and D. P. Brown, 2005a: Tropical cyclone report: Hurricane Katrina (23-30 August 2005). Tech. Rep., National Hurricane Center, National Oceanographic and Atmospheric Administration, 43 pp. [Available online at http://www.nhc.noaa.gov/pdf/TCR-AL122005_Katrina.pdf.]

____, ____, and ____, 2005b: Tropical cyclone report: Hurricane Rita (18-26 September 2005). Tech. Rep., National Hurricane Center, National Oceanographic and Atmospheric Administration, 33 pp. [Available online at http://www.nhc.noaa.gov/pdf/TCR-AL182005_Rita.pdf.]

Lhermitte, R. M., and D. Atlas, 1961: Precipitation motion by pulse Doppler radar. *Proc. Ninth Weather Radar Conf.,* Kansas City, MO, Amer. Meteor. Soc., 218-223.

O'Bannon, T., 1985: Validation of the NEXRAD Wind Profiling (VAD) Algorithm. Memo to Anthony Durham (NEXRAD) Joint System Program Office) dated 12 July 1985, 9 pp.

Rabin, R. M., and D. S. Zrnic, 1980: Subsynoptic-scale vertical wind revealed by dual Doppler radar and VAD analysis. *J. Atmos. Sci.,* **37,** 644-654.

FHM-11, 1991: *Doppler Radar Meteorological Observations. Part C – WSR-88D Products and Algorithms.* Federal Meteorological Handbook No. 11, Office of the Federal Coordinator for Meteorological Services and Supporting Research, Washington, DC.

Wood, V. T., and R. A. Brown, 1992: Effects of radar proximity on single-Doppler velocity signatures of axisymmetric rotation and divergence. *Mon. Wea. Rev.,* **120,** 2798-2807.

TABLE 1. VAD algorithm outputs of altitude (ALT), wind direction (DIR), wind speed (SPD), RMS, slant range (SRNG), elevation angle (ELEV), number of terms (TERM) in the polynomial regression, azimuthal angle difference (ΔAZ) between the locations of extreme Doppler velocity values, and number of fit (FIT) tests at 1300 UTC on 29 August 2005. Asterisk (*) represents erroneous wind direction due to the lack of data points in the weak-reflectivity regions between two adjacent rainbands and/or between an eyewall and adjacent rainband.

WSR-88D VAD Algorithm						Experimental VAD Algorithm					
ALT (kft)	DIR (deg)	SPD (kt)	RMS (kt)	SRNG (nm)	ELEV (deg)	DIR (deg)	SPD (kt)	RMS (kt)	TERM	ΔAZ (deg)	FIT
09	081	103	8.5	13.7	6.0	076	106	2.9	7	166	2
14	078	094	8.6	13.2	9.9	073	091	3.5	7	163	2
35	077	063	9.6	17.1	19.5	054*	055	3.2	6	144	1
40	078	044	9.4	19.5	19.5	057*	049	2.8	7	147	2
45	067	048	5.9	22.0	19.5	070	042	3.6	6	160	1

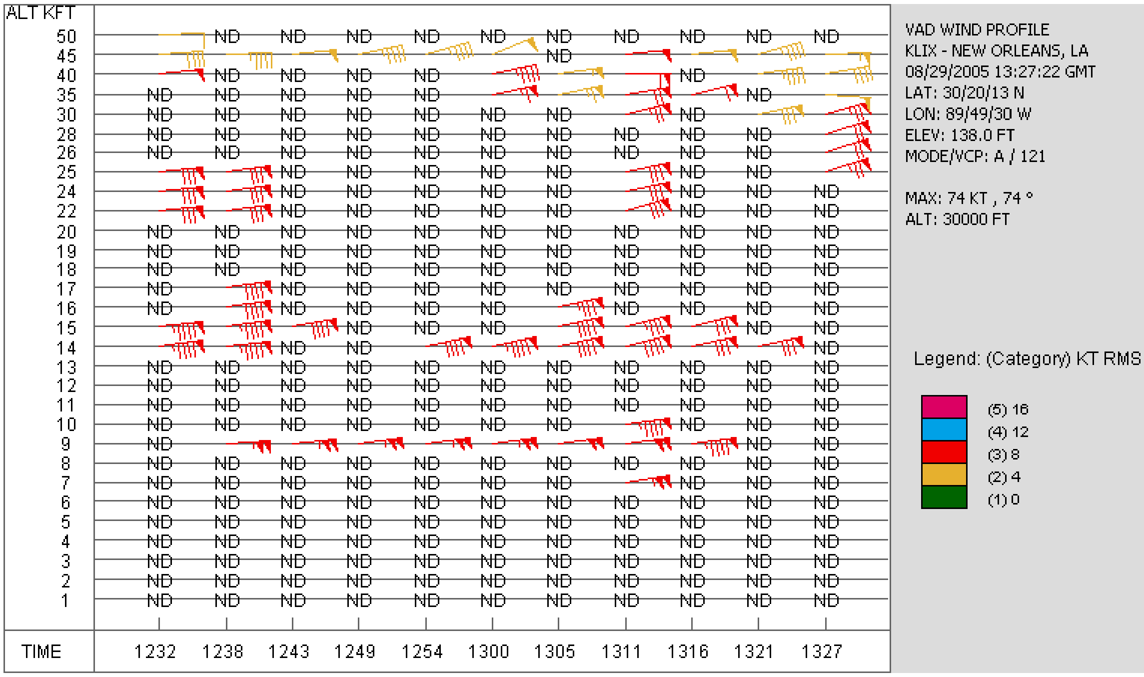

Fig. 1. VWP for the New Orleans/Slidell WSR-88D (KLIX) on 29 August 2005 during the approach of Hurricane Katrina. Abscissa is UTC time and ordinate is height MSL in kft. ND represents no data. The wind plotting convention is flag, 50 kt; barb, 10 kt; and half-barb, 5 kt. Wind vectors are colored according to the RMS difference (shown in the lower, right portion) between Doppler velocity measurements and fitted sine curve on the VAD display.

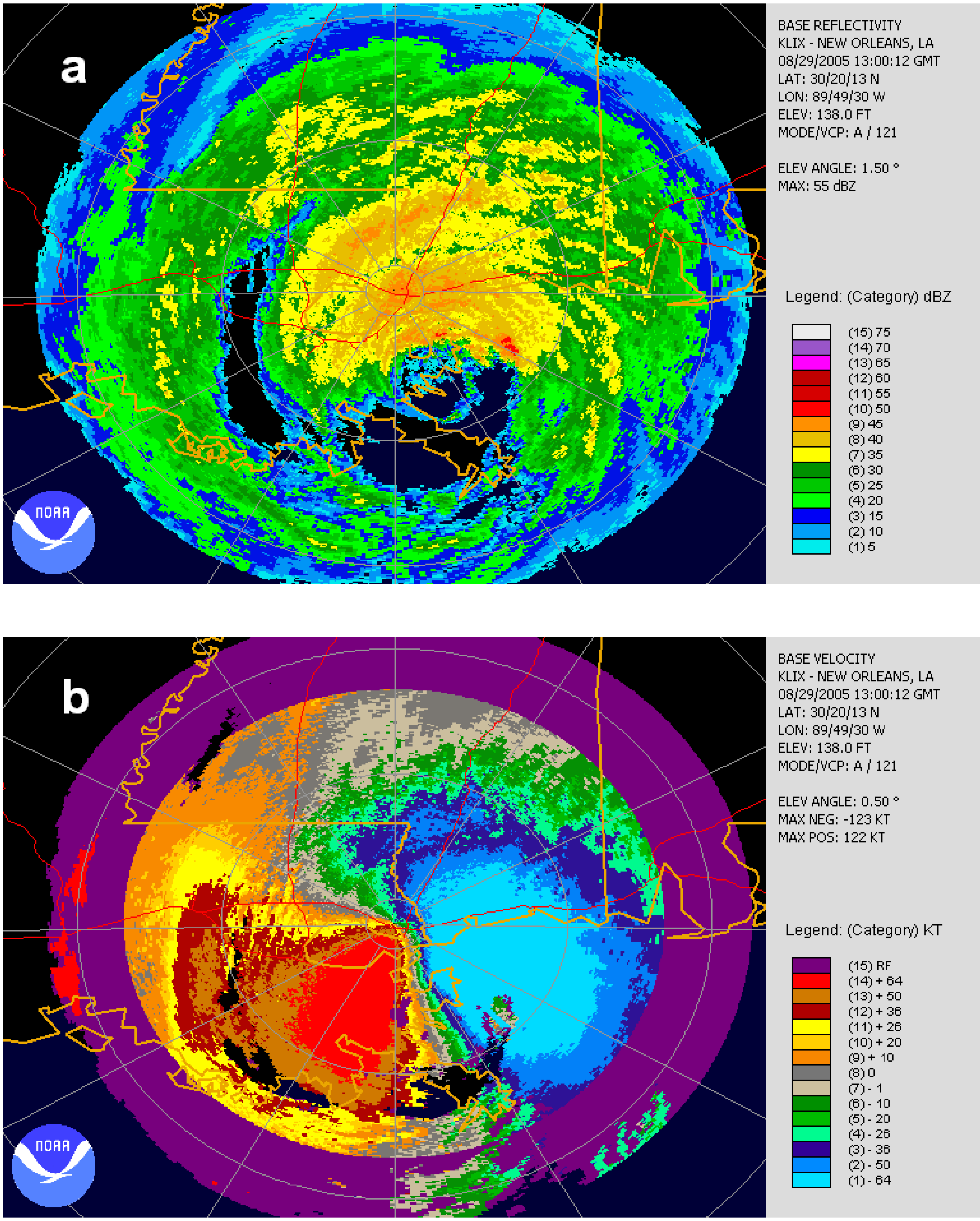

Fig. 2. New Orleans/Slidell WSR-88D (KLIX) displays of (a) reflectivity at 1.5º elevation angle and (b) Doppler velocity at 0.5º elevation angle with VCP 121 at 1300 UTC on 29 August 2005 during the approach of Hurricane Katrina. Range rings are separated by 50 n mi. The gray inner circle is 10 n mi. Orange boundaries represent state line; red lines represent Interstate highways. In (a), reflectivity values are color-coded on the right. In (b), Doppler velocity values are color-coded on the right; the magenta areas represent missing data owing to overlaid range-folded echoes.

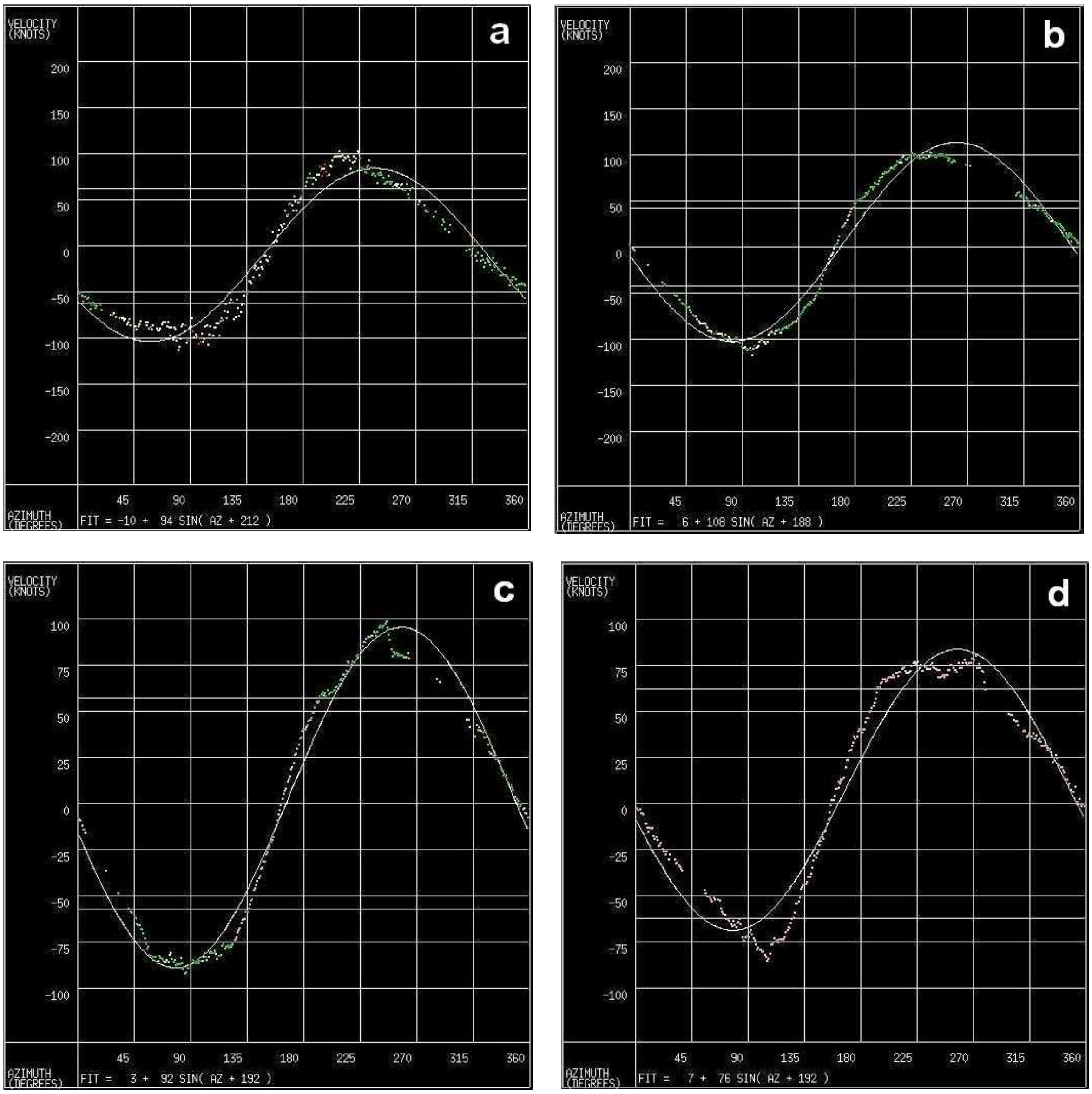

Fig. 3. Velocity (ordinate)-Azimuth (abscissa) Display at (a) 2 kft MSL (1.5º elevation angle at slant range of 11.1 n mi with VCP 121), (b) 8 kft (4.3º elevation angle at slant range of 16.8 n mi), (c) 14 kft (9.9º elevation angle at slant range of 13.1 n mi), and (d) 22 kft (14.6º elevation angle at slant range of 14.1 n mi) as measured by New Orleans/Slidell WSR-88D KLIX at 1300 UTC on 29 August 2005. RMS difference between Doppler velocity measurements and the fitted sine curve is (a) 16 kt, (b) 13 kt, (c) 9 kt, and (d) 12 kt.

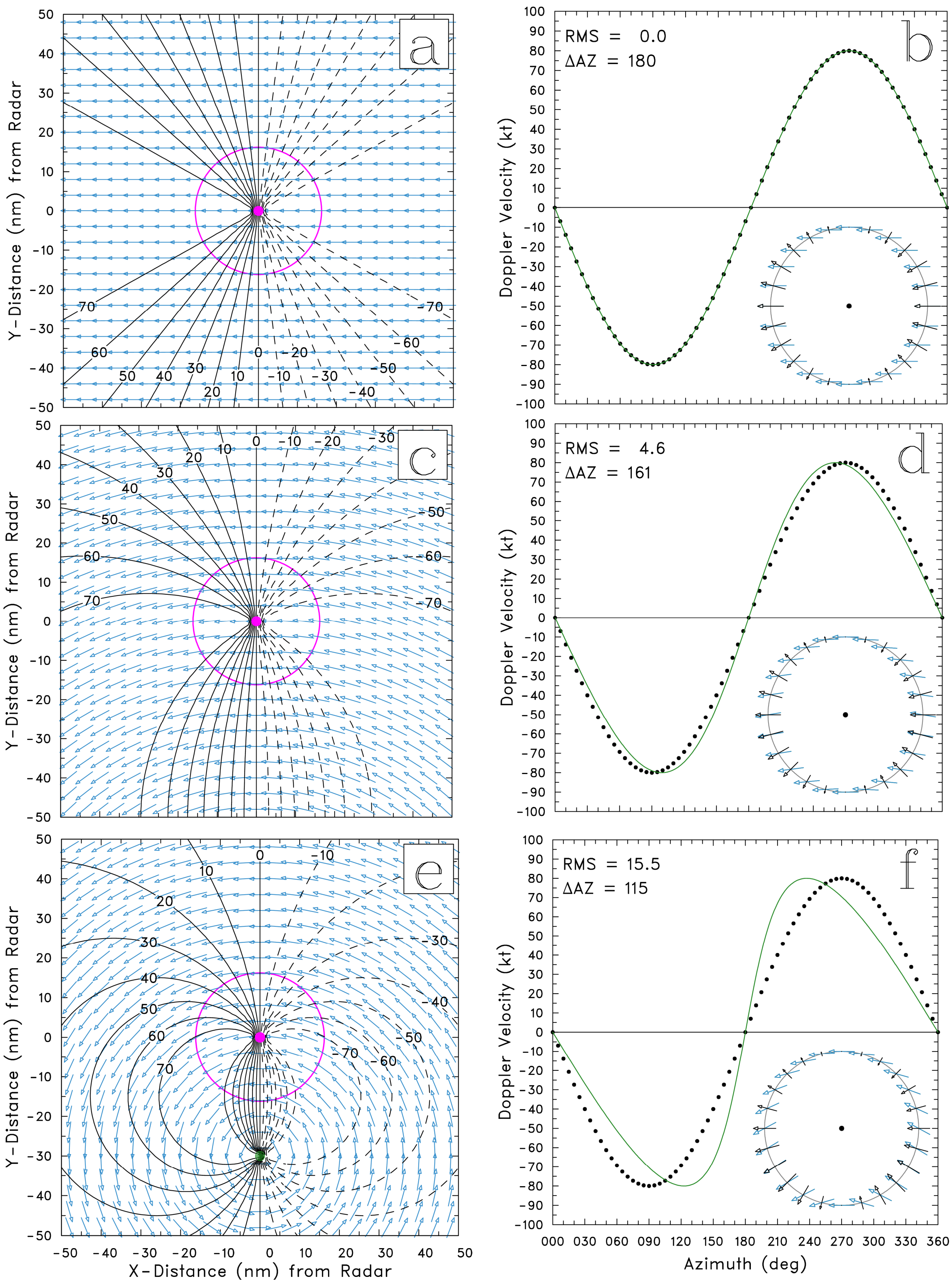

Fig. 4. Simulated hurricane (blue) wind vectors at (a) >1000, (c) 100, and (e) 30 n mi from a simulated Doppler radar center (magenta dot). In (e), a green hurricane center is located at 30 n mi of the radar. Magenta VAD circle is at 16.2 n mi. Positive and negative Doppler velocity values corresponding to hurricane winds are indicated by solid and dashed contours, respectively. (b), (d), (f) Simulated VAD first-order sine curve (black dotted curve) corresponds to uniform wind field blowing from east to west across the VAD circle. Simulated VAD quasi-sine curve (green solid

curve) corresponds to nonuniform wind field across the VAD circle. ΔAZ *is the azimuthal angle difference between the locations of maximum and minimum Doppler velocity values on the VAD circle. RMS is the root-mean-square difference between the black dotted data points and the green solid curve. Blue and black wind vectors, respectively, represent hurricane winds and Doppler radial components of hurricane winds distributed on the gray VAD circle.*

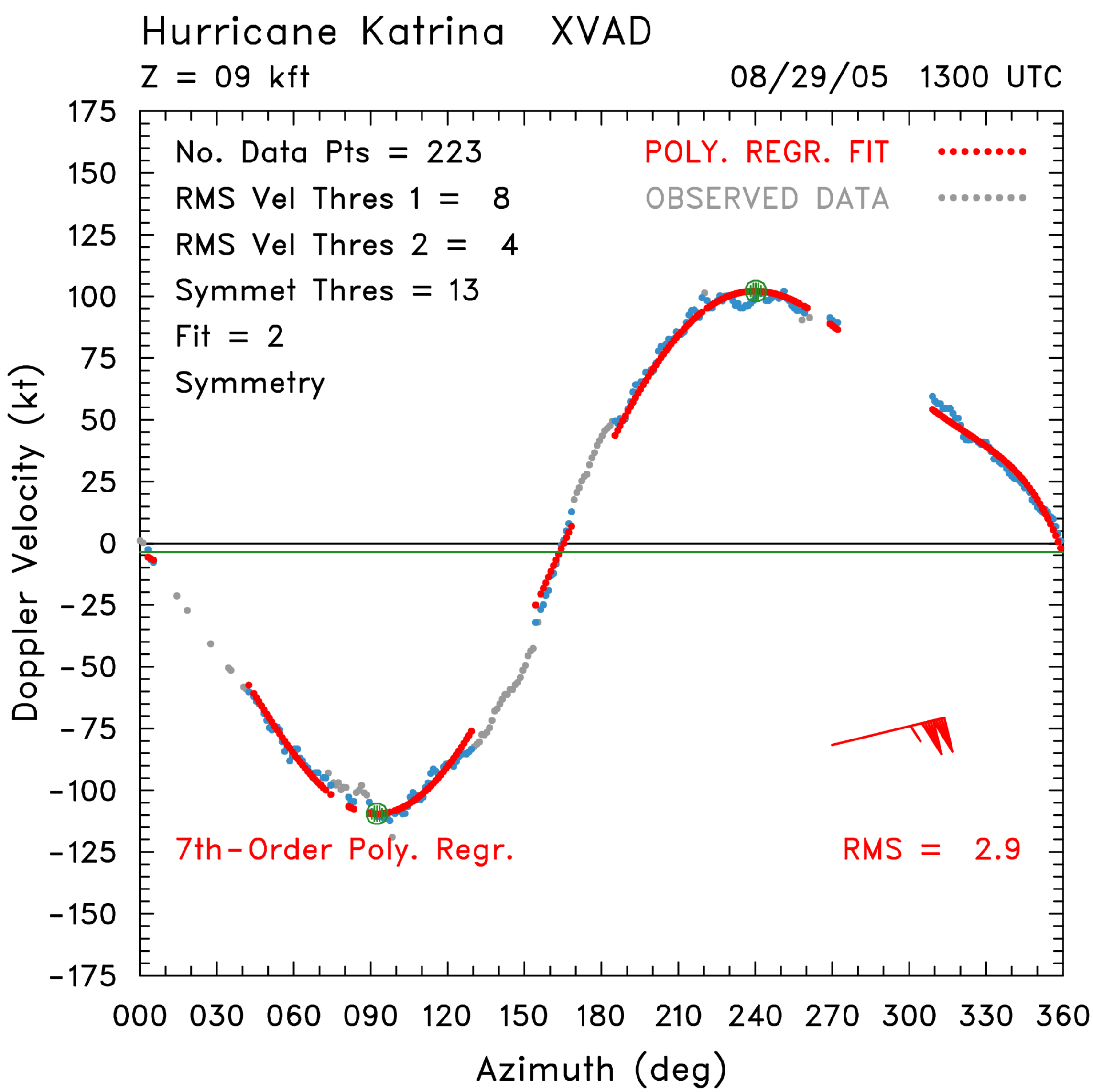

Fig. 5. Experimental Velocity (ordinate)-Azimuth (abscissa) Display (XVAD) at 9 kft MSL as measured by New Orleans/Slidell WSR-88D KLIX at 1300 UTC on 29 August 2005 during the approach of Hurricane Katrina. Gray data points represent original data points; blue dots represent remaining data points after being filtered out. Red dots represent polynomial data points. Large green dots represent the locations of azimuths where extreme Doppler velocity values occur. Green horizontal line is the vertical offset from zero Doppler velocity value.

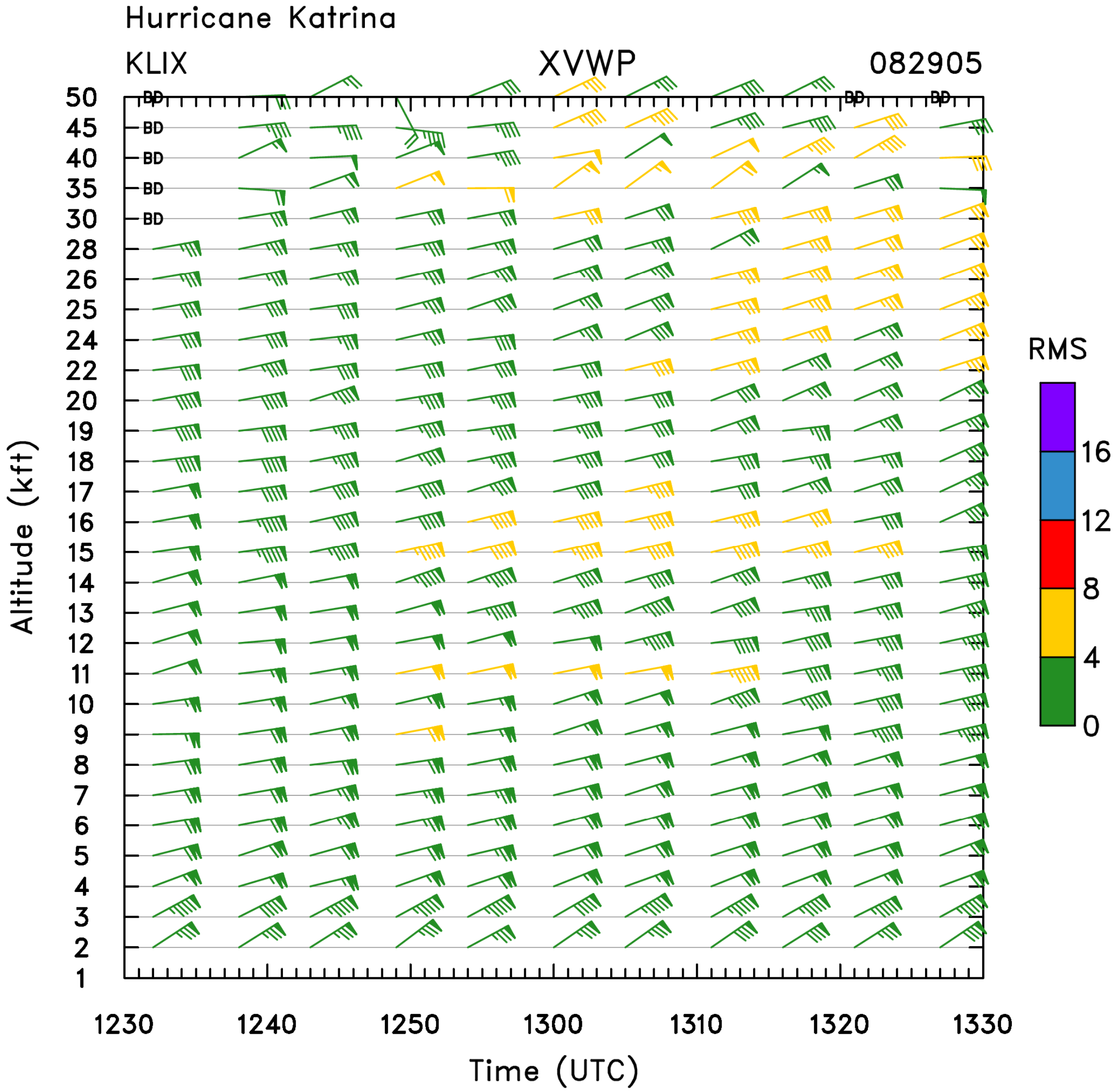

Fig. 6. Same as Fig. 1, except that the XVWP has been reconstructed by polynomial regression technique. BD represents bad data.

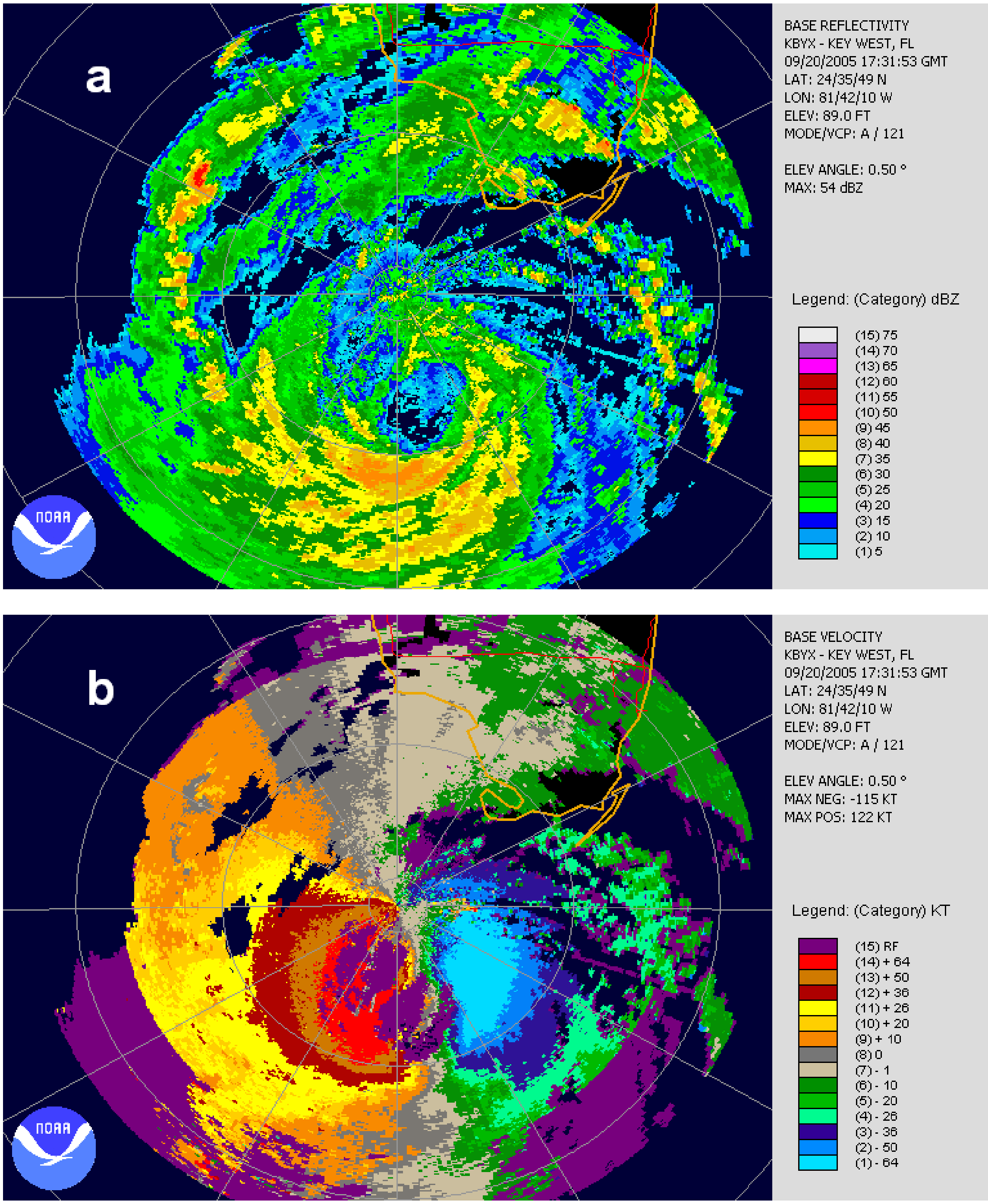

Fig. 7. Same as Fig. 2, except for the Key West WSR-88D (KBYX) at 0.5º elevation angle at 1731 UTC on 20 September 2005 during the passage of Hurricane Rita.

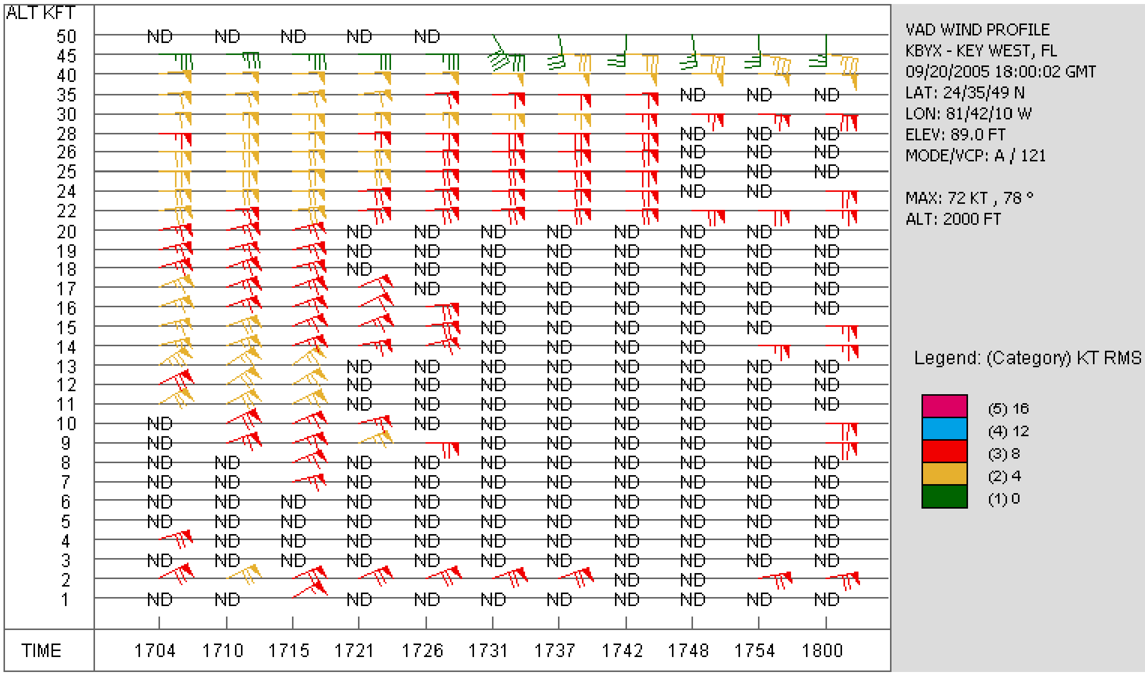

Fig. 8. Same as Fig. 1, except for the Key West WSR-88D (KBYX) on 20 September 2005 during the passage of Hurricane Rita.

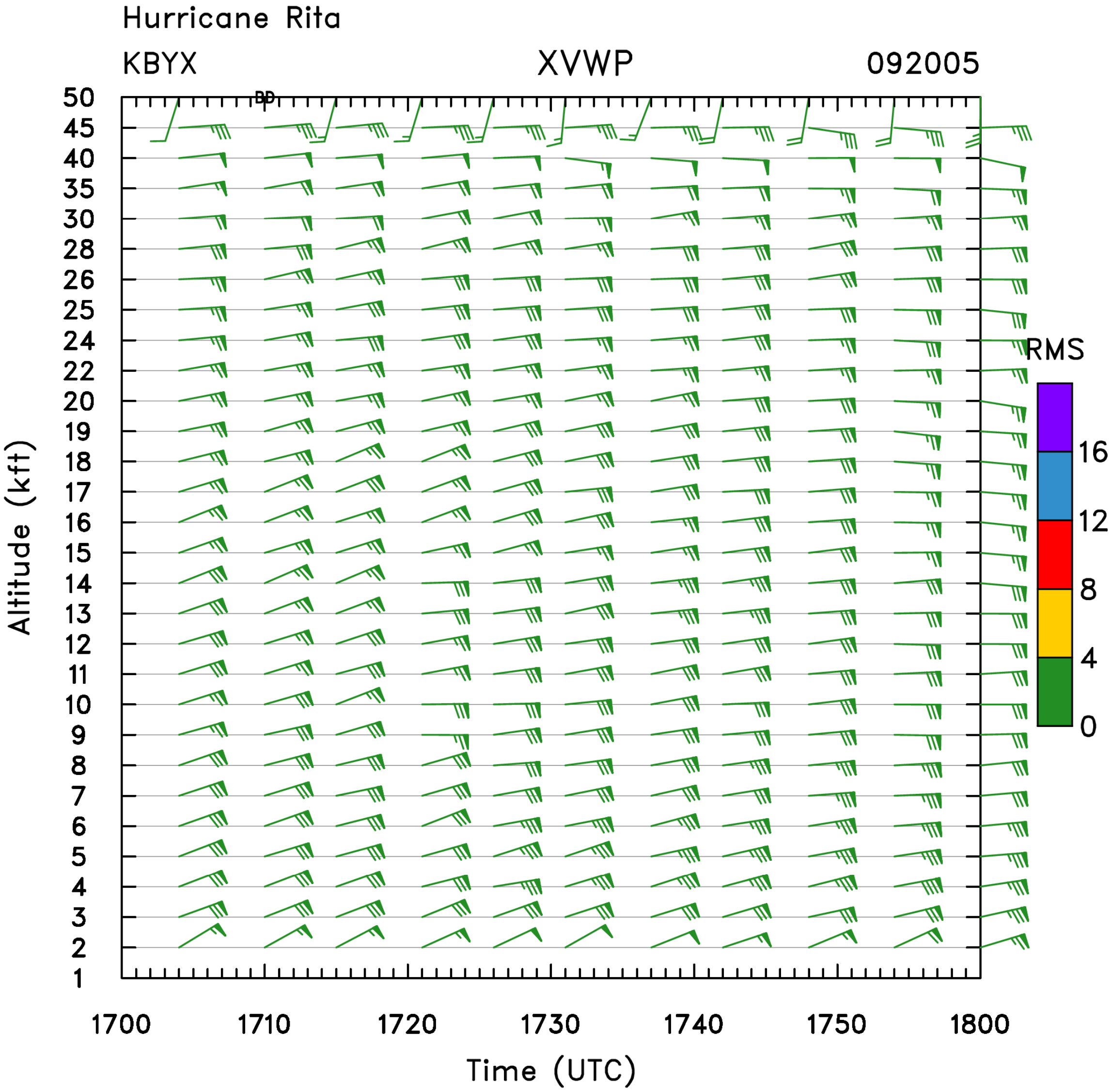

Fig. 9. Same as Fig. 6, except for the Key West WSR-88D (KBYX) on 20 September 2005 during the passage of Hurricane Rita.